

## Some Low-Field Transport Properties of LPE-grown GaAs and AlAs Mixed Alloys and Saxena's Deep Donor

A.K. Saxena

*Department of Electronics and Computer Engineering  
University of Roorkee, Roorkee-247 667*

### ABSTRACT

*GaAs* and *AlAs* mixed crystals offer the possibilities of their potential applications in various modern optical, electrical and microwave heterostructure devices to realize complete systems performing various operations for both civil and defence operations. For  $x \geq 0.25$ , a deep level, known as Saxena's deep donor dominates the electrical characteristics of  $Ga_{1-x}Al_xAs$  crystals and its activation energy increases with  $x$ , being 0.170 eV at  $x \approx 0.44$ . For  $x > 0.44$ , the energy of this level below the  $X$  minima decreases with  $x$ , reaching a value of 0.106 eV at  $x = 0.78$ . The results show that the lowest energy indirect minima is  $L$  in *GaAs* lying 0.280 eV above the  $\Gamma$  minimum and the  $\Gamma-L$  cross-over composition is  $x = 0.47$ . A long lifetime ( $T < 50$  K) photoconductivity effect is also observed, which is associated with the indirect nature of the deep level. An increase in photo-Hall mobility at low temperatures over the dark mobility shows that this level has the properties of an acceptor-like centre. Shallow donor levels are also present in the crystals, but are heavily compensated. The Hall to drift mobility ratio peaks near the direct-indirect minima cross-over composition and has a peak value of  $\sim 3.8$  at  $x = 0.42$ .

### 1. INTRODUCTION

Many electronic systems in civil and defence make use of various semiconductor devices i.e., optical, electrical, microwave etc. Because of superior material properties, 3-5 group compound devices have taken over silicon devices. Modern versions of these devices employ 3-5 group binary, ternary and quaternary compounds in heterostructure configurations. The potential defence applications of these devices could be in making portable radars, satellite and wide band communication systems using optical fibre technology, various electronic control parts of missiles etc. In the limited space available for a research paper, it is not possible to highlight all the applications of 3-5 semiconductors devices but I will quote their use in optical fibre communication system as an example. This technology provides significant improvements in telephone systems, computers and instrumentation. Such systems will have many advantages over conventional systems such as (i) minimization of

electromagnetic interference, (ii) low weight, (iii) low losses, and (iv) potential long link capabilities extending to GHz range etc.

For efficient transmission, the fibre should be excited by an optical source (laser) in the wavelength range  $\sim 0.8 - 0.9 \mu\text{m}$  where the absorption losses and dispersion are low, allowing high fidelity transmission over long distances. It is, therefore, imperative to choose a semiconductor with not only the right band-gap but with also a direct energy band-gap for efficient optical emission. Similarly, at the receiving end, a matching photodetector will be required. Also, the devices made from 3-5 group compounds are expected to work much faster due to higher carrier mobilities. Further, due to the requirement of lattice matching in heterostructure devices, the choice of semiconductors to which ternary and quaternary compounds can be grown are limited. With the advancement in technology of crystal growth, it is now possible to relax this requirement and grow thin strained layer super-lattice

structures which allow us more flexibility in band-gap engineering for specific devices applications. It is, therefore, necessary to study the material properties of  $Al_x Ga_{1-x}As$  which meets most of the requirements prior to device design and fabrication.

The electrical properties of several III-V semiconductor alloys are being investigated because of their potential applications in electroluminescent devices, such as LED's, solar cells, DH lasers and microwave devices. The  $Ga_{1-x} Al_xAs$  alloy system is perhaps the most important technologically because of the lowest lattice mismatch ( $\sim 0.16$  per cent) between  $GaAs$  and  $AlAs$ <sup>1</sup> as compared to other ternary alloys. The occurrence of current saturation in ternary III-V compounds has been reported by Majerfeld and Pearson<sup>2</sup> and for  $Ga_{1-x} Al_xAs$  by Immorlica and Pearson<sup>3</sup> and Sugeta *et al.*<sup>4</sup>. A double velocity heterostructure  $Ga_{1-x} Al_xAs/GaAs$  microwave device proposed recently<sup>5</sup> is based on the reduced value of the electron saturation velocity in a mixed alloy relative to that in  $GaAs$ . However, the value of the saturated velocity against electric field is not known in detail because of lack of knowledge of the Hall to drift mobility ratio.

A new ordering and the energies for the indirect  $L$  and  $X$  conduction band minima in  $GaAs$  have been proposed by Aspnes<sup>6</sup> from optical absorption and electroreflectance measurements. Adams *et al.*<sup>7</sup> analysed pressure dependence of the velocity field characteristic for  $GaAs$  by means of Monte Carlo simulations and concluded that the relative energy positions of the  $L$  and  $X$  valleys given by Aspnes were necessary to explain the pressure data. To interpret the low temperature optical measurements on  $Ga_{1-x} Al_xAs$ , Dingle *et al.*<sup>8</sup> also used the ordering proposed by Aspnes for the indirect minima in  $GaAs$ . However, neither has a transport determination of the  $\Gamma-L$  energy separation in the  $Ga_{1-x} Al_xAs$  alloys been reported nor has the effect of the hydrostatic pressure on the electrical properties been shown.

Deep levels, be they radiative or non-radiative, play an important role in limiting the performance of semiconductor devices. Observed degradation phenomenon in  $Ga_{1-x} Al_xAs$  lasers have been attributed to dislocations, defects and radiative and non-radiative deep centres<sup>9-13</sup>. In order to evaluate the merits of  $Ga_{1-x} Al_xAs$  for various device applications, it is necessary to detect and characterise deep levels which may be

present. To the author's knowledge, no exhaustive study of deep levels in  $Ga_{1-x} Al_xAs$  has been reported so far. Springthorpe *et al.*<sup>9</sup> showed that deep levels are present in  $Te$ -doped  $Ga_{1-x} Al_xAs$  and suggested that its activation energy as a function of  $x$  follows the indirect  $L$  minima.

Nelson<sup>10</sup> observed the long lifetime ( $\tau \sim$  hours,  $T \leq 60$  K) photoconductivity effect in  $Te$ -doped  $Ga_{1-x} Al_xAs$  and concluded that a potential barrier to electron capture is associated with the deep (donor) level. It has not been shown from the past work that deep levels in  $Ga_{1-x} Al_xAs$  are associated with the indirect minima at  $L$  and  $X$  points in the Brillouin zone, rather than the lowest energy  $\Gamma$  minimum at the zone centre, as is assumed *a priori*.

In this paper, we have investigated the activation energy of the deep levels in  $Ga_{1-x} Al_xAs$  by means of Hall effect measurements as a function of temperature and hydrostatic pressure for crystals with composition in the range  $0 < x < 0.78$ . The position of the  $L$  conduction band minima is determined for alloy compositions  $0.19 < x < 0.61$  and the alloy composition at which the  $\Gamma-L$  minima are equal in energy is also established. Photo-Hall measurements have been made to investigate the donor or acceptor-like nature of the deep levels. Also, the Hall to drift mobility ratio has been determined at 300 K as a function of alloy composition.

## 2. EXPERIMENTAL

### 2.1 Samples

The high purity  $Ga_{1-x} Al_xAs$  layers used in the present investigation were grown on semi-insulating  $GaAs$  substrates by liquid phase epitaxy and had a thickness of 5-10  $\mu m$  and room temperature carrier concentration of  $5-10 \times 10^{15} cm^{-3}$ . The alloy compositions were determined by converting measured room temperature cathodoluminescence band-gap energies into compositions by means of the energy gap composition curve given by Panish<sup>11</sup>. Clover leaf patterns were delineated on the surfaces of the epitaxial layers using photolithographic techniques. Four  $Sn$  contacts were alloyed at 600 °C for 2 min in  $H_2$  atmosphere on the four leaves and near to the periphery of the clover leaf pattern. For Hall measurements as a function of pressure and temperature, the samples were prepared using Bridgmann rings and epoxy resin as the pressure transmitting medium<sup>12</sup>.

## 2.2 Measurements

Hall measurements as a function of temperature ( $T < 300$  K) were made using an air produce Displex (DE-202) system which utilises liquid *He* as the cooling agent. The temperature of the sample could be controlled within  $\pm 0.1$  K for an indefinite period of time. The Hall and resistivity measurements were made by reversing the directions of currents through the contacts and the magnetic field and an average used in order to eliminate the contact effects. A constant current generator was used to provide the sample current and a reasonable current density was used to avoid heating of the samples. All the voltages were accurately measured on an electrometer with a high input impedance. Samples were exposed to white light filtered through a *Ge* filter for photo-Hall measurements. For measurements above room temperature, another system was used. It consisted of an OFHC copper block housing a heater element. The sample was held on top of the plate with four phosphorbronze metallic shoes which also provided electrical contacts to the alloyed *Sn* contacts on the epitaxial layers. The temperature of the sample could be controlled within  $\pm 1$  K and  $H_2$  gas was passed on to the sample at a reasonable rate to avoid the oxidation of the sample and other metal parts. Care was taken to avoid temperature gradients across the samples.

## 3. RESULTS

### 3.1 Hall Carrier Concentration ( $n_h$ ) as a Function of Composition at 300 K

The measured values of  $n_h$  at 300 K as a function of alloy composition are plotted in Fig. 1. It is seen that  $n_h$  decreases with  $x$  ( $0 < x < 0.37$ ), goes through a minimum at  $x \approx 0.37$  and then increases again for  $x > 0.37$ . The minimum in  $n_h$  occurs a few % of *Al* before the  $\Gamma$  and *X* minima are equal in energy<sup>13</sup>, showing that the  $\Gamma$ -*X* cross-over composition is greater than  $x \approx 0.37$ . The decrease in  $n_h$  with composition in the range  $0 < x < 0.37$  occurs due to electron transfer from the high mobility and low density of states  $\Gamma$  minimum to the low mobility and high density of states subsidiary minima as the separation between these minima decreases with  $x$ . For  $x > 0.37$ , a significant density of the electrons is transferred to the *X* minima and  $n_h$  increases with  $x$ . When the electron transfer to the *X* minima is complete,  $n_h$  is nearly equal to the electron concentration in the *X* minima and stays almost constant with  $x$ .

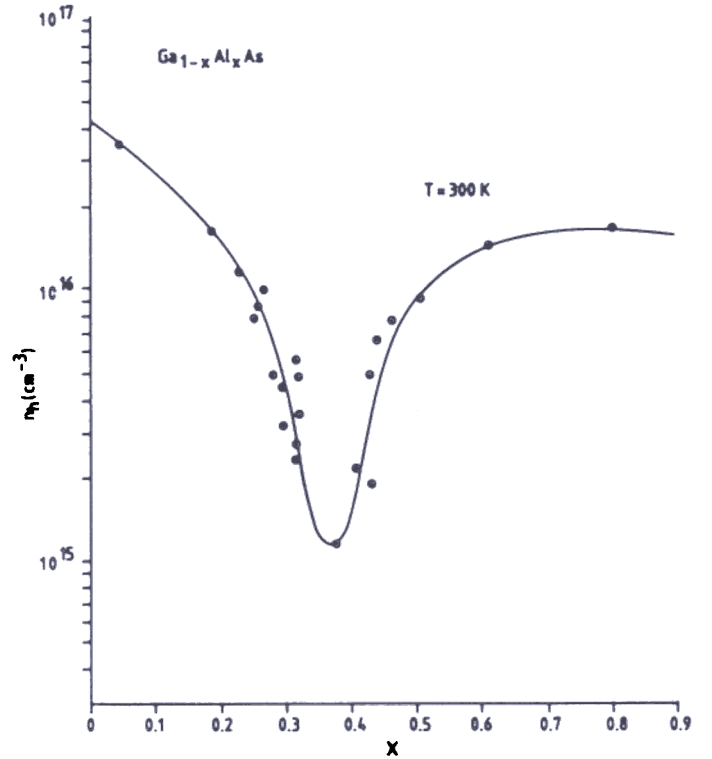


Figure 1 Hall carrier concentration at 300 K as a function of alloy composition.

### 3.2 Temperature Dependence of Hall and Photo-Hall Carrier Concentration

The temperature dependence of  $n_h$  for samples with alloy compositions in the range  $0 < x < 0.78$  has been studied and the results for a few compositions are shown in Fig. 2. The temperature dependence of photo-Hall carrier concentrations for a few compositions is also shown in Fig. 2. For crystals with  $x = 0.61$  and  $0.78$ , measurements were not possible for the samples in the dark for  $T < 83$  and  $45$  K, respectively, because of the high resistivities of the samples below these temperatures. No hysteresis effects are observed in  $n_h$  if the samples are cooled in the dark and the temperature then increased back to the room temperature. Full circles show the measured  $n_h$  values for samples in the dark and for decreasing temperature. Open circles represent the measured  $n_h$  values in the dark with increasing temperature after the samples were cooled down in the dark. After the samples are cooled down to the lowest temperature at which  $n_h$  can be measured, the samples are exposed to filtered radiation. The intensity of the radiation is increased until the photo-Hall voltage and the resistivity of the samples get almost saturated. For all the samples studied, persistent

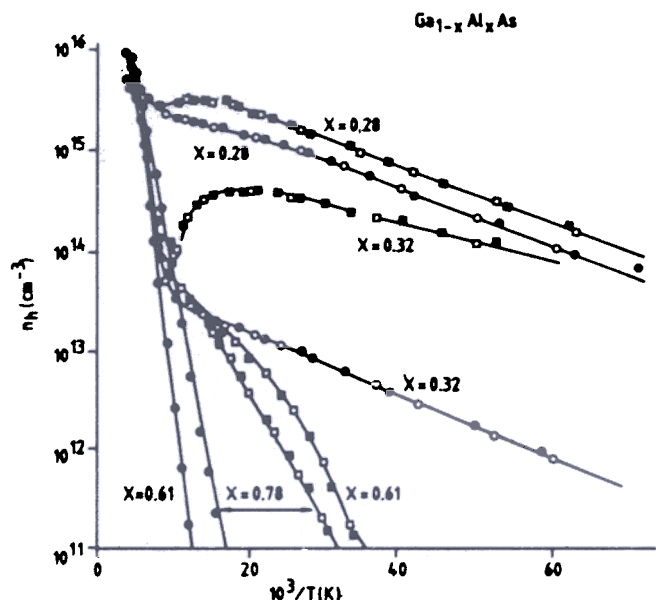


Figure 2. Temperature dependence of Hall and photo-Hall carrier concentrations for various alloy compositions. ( $\bullet$ ,  $\circ$ , measured Hall carrier concentrations in the dark for decreasing and increasing temperatures;  $\blacksquare$ , optical excitation at 16 K with white light filtered through a Ge filter and for increasing temperature both with and without the optical source;  $\square$ , constant optical excitation and decreasing temperature).

photoconductivity with increase in  $n_h$  is observed for hours at low temperatures ( $T < 50$  K) even without the optical source and so long as the temperature of the sample is maintained constant. No changes in  $n_h$  can be detected with increasing temperature and with or without the optical source. Data corresponding to filtered radiation are represented as full squares. Open squares show the measured  $n_h$  values for decreasing temperature and for constant optical excitation. The photoconductivity can be quenched only at a high temperature, where  $n_h$  for samples under or after optical excitation equals  $n_h$  measured in the dark. For crystals with alloy compositions  $x = 0.28$  and  $0.32$ , the slope of  $n_h$  with  $1/T$  for  $T \lesssim 65$  K, after and with photoexcitation is almost the same as observed for samples in the dark. For samples with  $x = 0.61$  and  $0.78$  quasi-saturation in  $n_h$  with or without the optical source is observed for  $T \lesssim 100$  K, after these were cooled down in the dark.

The most striking feature of these curves is the sharp decrease in  $n_h$  for  $T < 300$  K. This occurs due to the deionisation of a deep level in the crystals. The rate of change of  $n_h$  with  $1/T$  increases with  $x$  and is found to be maximum for  $x \approx 0.44$ . For  $x > 0.44$ , the rate of change

of  $n_h$  with  $1/T$  decreases monotonically with  $x$ . The activation energy of the deep level is, therefore, expected to be maximum in the neighbourhood of  $x \approx 0.44$ . The Hall carrier concentration passes through a maximum at about the room temperature for crystals with  $x = 0.28$  and  $0.32$  because of carrier transfer to the higher energy subsidiary minima. The slope of  $n_h$  in the temperature range  $300 \text{ K} \lesssim T \lesssim 500 \text{ K}$  is a measure of the energy separation between the  $\Gamma$  minimum and the higher energy subsidiary minima involved in the carrier transfer process. At about 550 K,  $n_h$  value rises very sharply with temperature for crystals with  $x = 0.28$  and  $0.32$  due to electron conduction in the substrates.

### 3.3 Temperature Dependence of Hall Carrier Concentration for Various Applied Pressures

Temperature dependence of  $n_h$  for crystals of different alloy compositions and for various applied pressures has been measured. The results for crystals with  $x = 0.32$  are shown in Fig. 3: The slope of  $n_h$  with  $1/T$  initially increases with pressure and beyond 20 k bar decreases with pressure. The activation energy of the deep level, therefore, goes through a maximum as a function of pressure in a similar way as it is seen to be a function of alloy composition. The data clearly show that the deep level is associated with the indirect minima. If it was associated with the  $\Gamma$  minimum, then at pressures as high as 36 k bar where the  $X$  minima is the lowest in energy, this level would not have been seen.

### 3.4. Temperature Dependence of Hall and Photo-Hall Mobilities

The variation of Hall and photo-Hall mobilities with temperature is shown in Fig. 4 for a crystal with alloy composition  $x = 0.32$ . The symbols used have the same meanings as described in Section 3.2. An increase in the photo-Hall mobility at low temperatures compared to the dark value shows that an acceptor-like level is involved in photoexcitation.

## 4. ANALYSIS

### 4.1 Temperature Dependence of Hall Carrier Concentration

The results of temperature dependence of Hall carrier concentration are analysed on the basis of the following model. The energy levels at  $E_{D_1}$  and  $E_{D_2}$  are assumed to be the shallow and deep levels and the sharp

increase in  $n_h$  for  $T \geq 500$  K has been accounted for by including a third level at energy  $E_{D_3}$ . In the crystals studied,  $(N_D - N_A) < 10^{16} \text{ cm}^{-3}$  and, therefore, the number of electrons in the  $\Gamma$  and  $X$  minima are given by the equations:

$$n_{\Gamma} = N_c^{\Gamma} e^{E_F/kT} \quad (1)$$

$$n_X = N_c^X e^{(E_F - \Delta E_{\Gamma X})/kT} \quad (2)$$

$$n_L = N_c^L e^{(E_F - \Delta E_{\Gamma L})/kT} \quad (3)$$

where  $E_F$  is the Fermi energy and is obtained by satisfying charge neutrality condition for the model proposed above.  $\Delta E_{\Gamma X}$  and  $\Delta E_{\Gamma L}$  are the energy

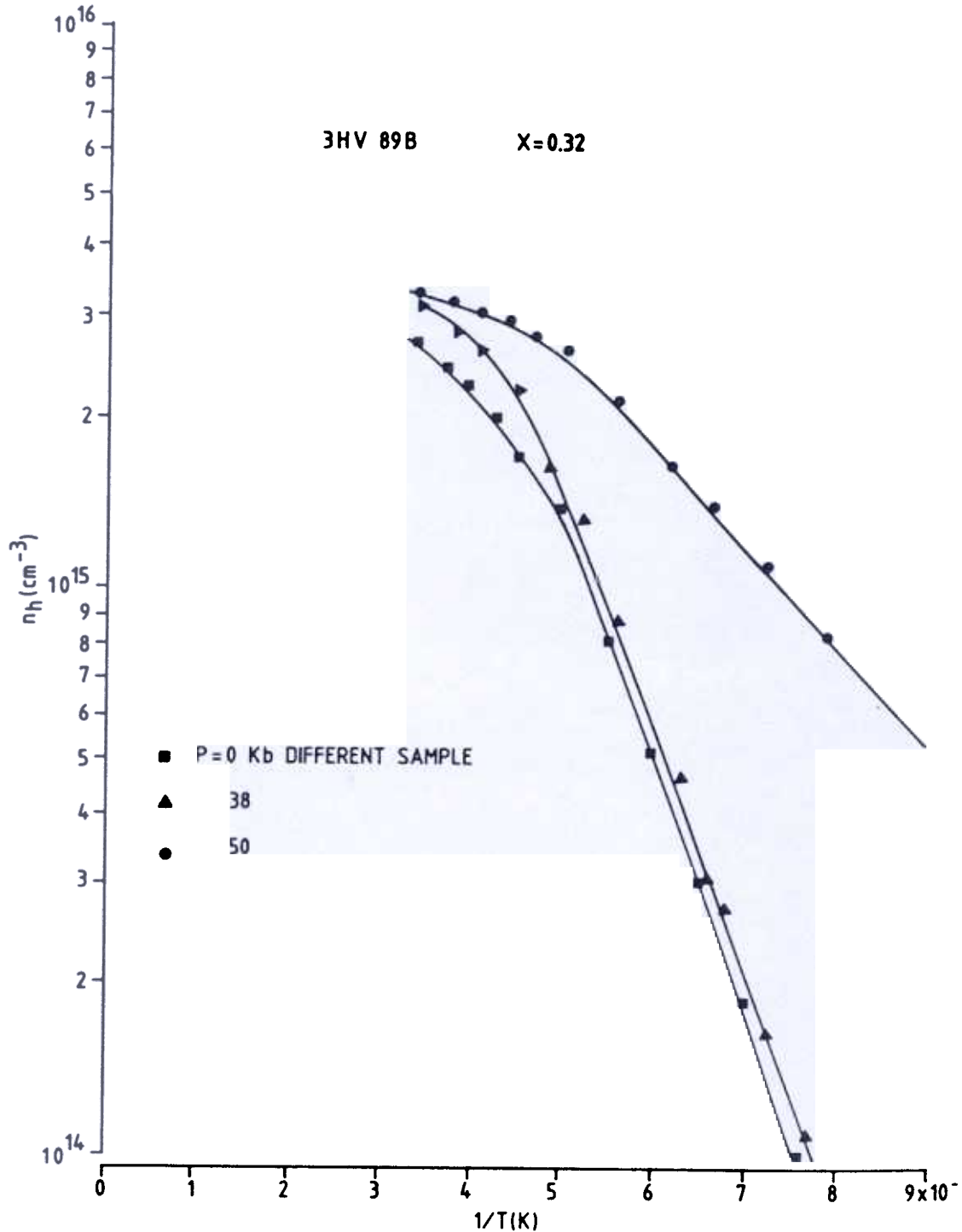


Figure 3. Temperature dependence of Hall carrier concentration for various applied pressures for crystal with  $x = 0.32$ .

separations between the  $\Gamma$ - $X$  and  $\Gamma$ - $L$  minima respectively.  $N_c$  is the density of states in the appropriate minima and is given by the equation:

$$N_c = \frac{4\sqrt{2}}{h^3} \pi (m_{\Gamma,L,X}^* kT)^{3/2}$$

where  $m^*$  is the electron effective mass. The equations for Hall coefficient  $R_H^{14}$ , mobility<sup>15</sup>,  $\mu_h$ , and drift mobility<sup>16</sup>,  $\mu_d$ , have been appropriately modified for a three-condition band material and are given by the equations:

$$R_H = \frac{1}{-e n_h} = \frac{[1 + (\frac{n_X}{n_\Gamma})(\frac{\mu_X}{\mu_\Gamma})^2 + (\frac{n_L}{n_\Gamma})(\frac{\mu_L}{\mu_\Gamma})^2]}{e n_\Gamma [1 + (\frac{n_X}{n_\Gamma})(\frac{\mu_X}{\mu_\Gamma}) + (\frac{n_L}{n_\Gamma})(\frac{\mu_L}{\mu_\Gamma})]} \quad (4)$$

$$\mu_h = \frac{\mu_\Gamma [1 + (\frac{n_X}{n_\Gamma})(\frac{\mu_X}{\mu_\Gamma})^2 + (\frac{n_L}{n_\Gamma})(\frac{\mu_L}{\mu_\Gamma})^2]}{[1 + (\frac{n_X}{n_\Gamma})(\frac{\mu_X}{\mu_\Gamma}) + (\frac{n_L}{n_\Gamma})(\frac{\mu_L}{\mu_\Gamma})]} \quad (5)$$

$$\mu_d = \frac{\mu_\Gamma [1 + (\frac{n_X}{n_\Gamma})(\frac{\mu_X}{\mu_\Gamma}) + (\frac{n_L}{n_\Gamma})(\frac{\mu_L}{\mu_\Gamma})]}{[1 + \frac{n_X}{n_\Gamma} + \frac{n_L}{n_\Gamma}]} \quad (6)$$

where  $n_{\Gamma,L,X}$  and  $\mu_{\Gamma,L,X}$  are the carrier concentrations and mobilities in the  $\Gamma$ ,  $L$  and  $X$  minima, respectively.  $n_h$  and  $e$  are the Hall carrier concentration and electronic charge respectively. From Eqns (4) – (6), the ratio of the Hall to drift mobility is calculated as:

$$\frac{\mu_h}{\mu_d} = \frac{n_\Gamma + n_L + n_X}{n_h} \quad (7)$$

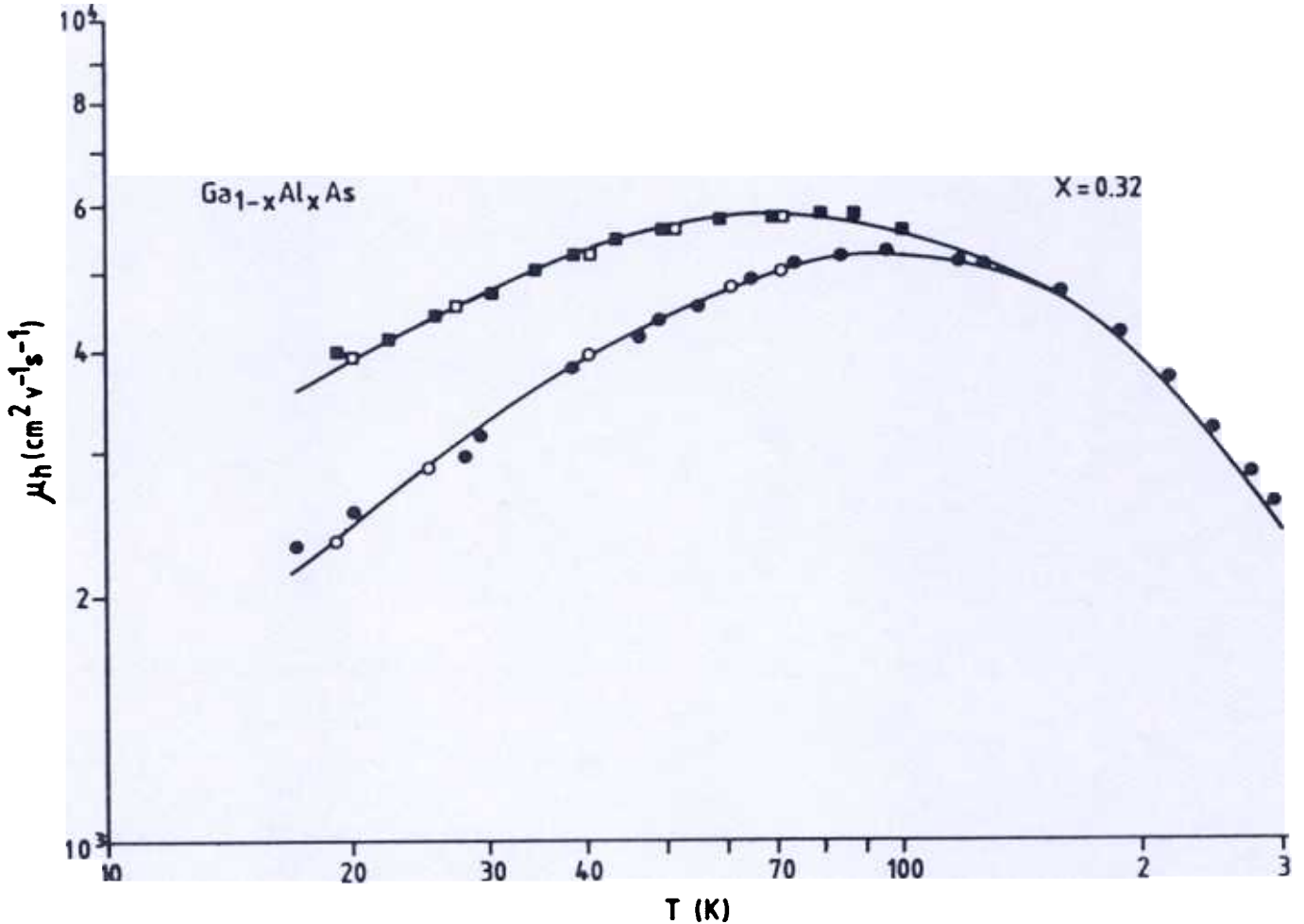


Figure 4. Temperature dependence of Hall and photo-Hall mobility for crystal with  $x = 0.32$  (●, ○, measured Hall mobility in the dark for decreasing and increasing temperatures respectively; ■, optical excitation at 16 K with white light filtered through a Ge filter for increasing temperature both with and without the optical source; □, constant optical excitation and decreasing temperature).

The variation of the electron mass in the  $\Gamma$  minimum as a function of  $x$  is calculated from the standard  $\vec{k} \cdot \vec{p}$  theory<sup>6</sup> and is given by the expression:

$$\frac{m_0}{m_\Gamma} = 1 + E_{p\Gamma} \left( \frac{2}{E_\Gamma} + \frac{1}{E_\Gamma + \Delta 0} \right) \quad (8)$$

where  $m_0$  and  $E_\Gamma$  are the free electron mass and the energy of the  $\Gamma$  minimum, respectively.  $E_{p\Gamma}$  and  $\Delta 0$  are the energies related to the momentum matrix element and the spin orbit splitting of the valence band, respectively. In  $Ga_{1-x}Al_xAs$ , the values of  $E_{p\Gamma}$  and  $\Delta 0$  are taken as 7.51 and 0.341 eV as given by Aspnes<sup>6</sup> for  $GaAs$  and are kept constant as a function of  $x$ . We considered  $m_\Gamma/m_0 = 0.067$  for  $GaAs$ <sup>17</sup>.

The density of states mass in the  $L$  minima is calculated from the Eqns<sup>6</sup>:

$$m_L^* = N^{2/3} m_t^{2/3} m_l^{1/3} \quad (9)$$

where  $N$  is the number of equivalent  $L$  minima and  $m_t$ ,  $m_l$ , the transverse and longitudinal masses of the minima. The mass  $m_l$  is also calculated from the  $\vec{k} \cdot \vec{p}$  theory<sup>6</sup> and is given by the equation:

$$\left( \frac{m_0}{m_l} \right) = 1 + 19.3 \left( \frac{1}{E_L} + \frac{1}{E_L + \Delta 1} \right) \quad (10)$$

where  $E_L$  and  $\Delta 1$  are the energies of the  $L$  minima and the spin orbit splitting of the valence band. In the present work,  $F_v = L_6^c - L_6^v = 3.041$  eV and  $\Delta 1 = 0.22$  eV are used as given by Aspnes for  $GaAs$ . Considering a longitudinal mass of  $1.9 m_0$  and  $N = 4^6$ , we obtain  $m_L^* = 0.55 m_0$ . The variation of  $m_L^*$  with  $E_L$  is calculated from Eqns (9) and (10). The density of states mass in the  $X$  minima of  $0.73 m_0$  is used, considering  $N = 3$  (ref. 6) and the mass in one minimum as  $0.35 m_0$  (ref. 18). The electron mass in the  $X$  minima is kept constant as a function of  $X$ , since the variation in the  $x$  minima energy is small compared to that of the  $\Gamma$  and  $L$  minima<sup>13</sup>. The mass  $m_X^* = 0.35 m_0$  is also consistent with the mobility calculations for the  $X$  minima in  $Ga_{1-x}Al_xAs$ <sup>13</sup>.

The mobility ratios  $\mu_X/\mu_\Gamma$  and  $\mu_\Gamma$  in Eqns (4)–(6) are treated independent of the temperature and the energy separation  $\Delta E_{\Gamma L}$  has a temperature coefficient of  $-5.4 \times 10^{-5}$  eV/K<sup>19</sup>. The electron mobility in the  $X$  minima has been measured for various alloy compositions ( $0.23 < x < 0.78$ ) and that in the  $L$  minima

has been obtained from Monte Carlo simulations<sup>13</sup>. The measured Hall mobility at 300 K for alloy compositions  $0 < x < 0.32$  is considered as the electron mobility in the  $\Gamma$  minimum, since for this composition range a majority of the electrons occupy this minimum. For  $x > 0.32$ ,  $\mu_\Gamma$  is also calculated from Monte Carlo simulations.

The energy separation between the  $\Gamma$ – $X$  minima for alloy compositions in the range  $0.23 < x < 0.38$  and the pressure coefficients of the  $\Gamma$ ,  $L$  and  $X$  minima have been determined<sup>13</sup> and the results will be published elsewhere. These coefficients are found to be  $12.6 \times 10^{-6}$ ,  $5.5 \times 10^{-6}$  and  $-1.5 \times 10^{-6}$  eV/bar for the  $\Gamma$ ,  $L$ , and  $X$  minima respectively and are used to determine the  $\Delta E_{\Gamma X}$  and  $\Delta E_{\Gamma L}$  at a particular pressure to calculate the energy of the deep level from the data shown in Fig. 3. The activation energies of the shallow and deep levels and the energy position of the  $L$  minima as a function of alloy composition are plotted in Fig. 5.

#### 4.2 Determination of Density of Optically Excited Centres

The electron capture and emission by the deep level in  $Ga_{1-x}Al_xAs$  essentially occur via the  $L$  conduction band minima for alloy compositions in the range  $0.25 < x < 0.32$  and via the  $L$  and  $X$  minima for  $0.32 < x < 0.36$ <sup>19</sup>. Also, for  $T \geq 100$  K, the electron capture time by the deep level is of the order of the time interval in which measurements are made, but for  $T < 100$  K, it can take several hours before the thermal equilibrium with respect to the deep level is reached. The thermal equilibrium statistics is applied to calculate the electron distribution in the shallow level, which is associated with the lowest energy minima. The Fermi energy and the density of electrons on the donor sites are given by the equations:

$$E_F = KT \ln \left( \frac{N_c}{n_c} \right)$$

and

$$n_d = \frac{N_D}{1 + F_{y2} \frac{E_{D1} - E_F}{KT}}$$

At low temperatures,  $n_c$  is taken as the measured  $n_h$  and  $N_D$  adjusted to satisfy the charge neutrality conditions for both Hall and photo-Hall  $n_h$ . The difference in the two donor densities so obtained is the density  $\Delta N$  of the optically excited centres in the band-gap and is tabulated in Table 1 for alloy compositions  $x = 0.28, 0.32$  and  $0.78$ .

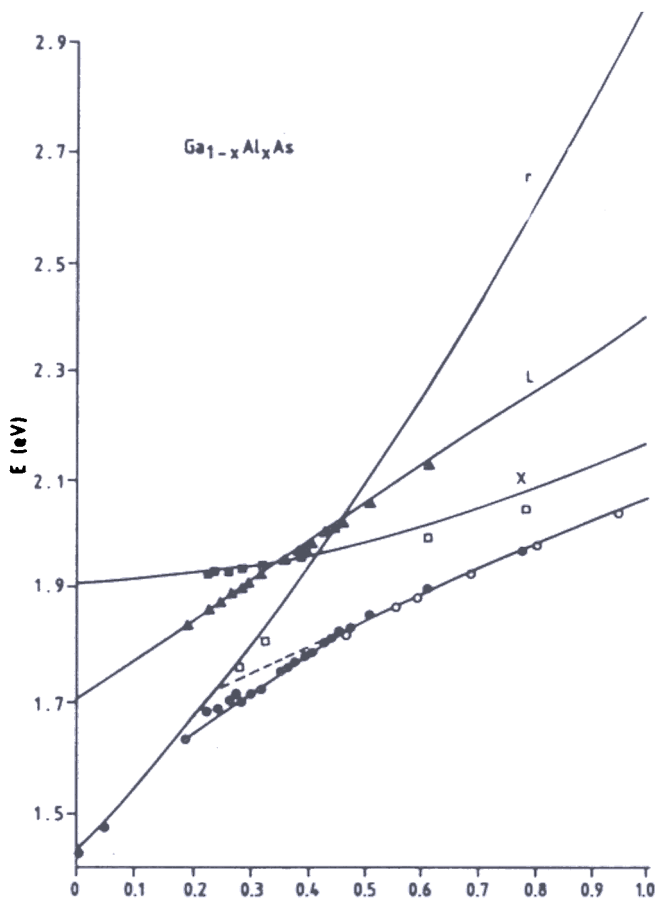


Figure 5. Deep levels and conduction band structure of  $Ga_{1-x}Al_xAs$ . (The curves labelled  $\Gamma$  (both in the direct and indirect gap regions) and  $X$  (in the indirect gap region) obtained from the data of Dingle *et al*<sup>8</sup> at 2 K, converted to 300 K using Varshni equation<sup>6</sup>. Curve labelled  $X$  (in the direct gap region) obtained from the pressure dependence of Hall coefficient in  $Ga_{1-x}Al_xAs$ <sup>13</sup>. Curve labelled  $L$  obtained from the present work. ●, □, shows the energy of the deep and shallow levels respectively as a function of composition; ○, energy of the deep level as a function of equivalent composition obtained by converting the pressure).

Table 1. Density  $\Delta N$  and  $\Delta N_I$  of optically excited centres (with white light filtered through a Ge filter) determined from the analysis of temperature dependence of Hall and photo-Hall carrier concentrations and mobilities respectively for crystals with various alloy compositions.

$x$	$\Delta N(\text{cm}^{-3})$	$\Delta N_I(\text{cm}^{-3})$
-----	----------------------------	------------------------------

### 4.3 Temperature Dependence of Hall and Photo-Hall Mobilities

The temperature dependence of the Hall and photo-Hall mobilities has been analysed using the following

scattering mechanisms: (i) polar optical scattering, (ii) acoustic mode scattering, (iii) equivalent intervalley scattering, (iv) piezo-electric scattering, (v) alloy scattering, (vi) space charge scattering, and (vii) ionised impurity scattering. Each scattering mechanism is considered independent of one another and the total mobility is calculated using Matthiessen's rule. All parameters involved in the calculations as a function of alloy composition have either been calculated or estimated from the values for other materials with similar band structures. The details of the analysis<sup>13</sup> will be published elsewhere. Values of density,  $\Delta N_I$ , of the optically excited centres are also tabulated in Table 1.

### 5. DISCUSSION

In Fig. 5, the energies of the  $\Gamma$  minimum ( $0 < x < 1.0$ ) and  $X$  minima (in the indirect gap region) as a function of alloy composition have been obtained by converting the data for the same as given by Dingle *et al*<sup>8</sup> at 2 K to that at 300 K using the Varshni equation<sup>6</sup>. The energy position of the  $X$  minima in the direct gap region has been obtained from the Hall coefficient maximum as a function of pressure<sup>13</sup>. The  $\Gamma$ - $X$  sub-band-gap in  $GaAs$  and the alloy composition at which these minima are equal in energy are found to be 0.485 eV and  $x = 0.43$ , respectively. The energies of the  $\Gamma$ ,  $X$  and  $L$  minima as a function of  $x$  at 300 K are best described by the equations:

$$E_{\Gamma} = 1.425 + 1.525x - 0.438x(1-x)$$

$$E_X = 1.9 + 0.26x - 0.16x(1-x)$$

$$E_L = 1.705 + 0.695x$$

By linearly extrapolating the  $L$  minima energy as a function of  $x$ , a value of 0.28 eV is obtained for the energy separation  $\Delta E_{\Gamma L}$  in  $GaAs$ . The alloy compositions at which the  $\Gamma$ - $X$  and  $\Gamma$ - $L$  minima are equal in energy are determined to be  $x = 0.43$  and 0.47, respectively. James and Moll<sup>20</sup> noted that the energy separation between the  $\Gamma$  and the next subsidiary minima had a probable best value of 0.33 eV at 300 K, but may be as low as 0.28 eV, which is the same as found for the  $\Gamma$ - $L$  separation in the present investigation. They also found a negative temperature coefficient for this separation, which is also consistent with the negative temperature coefficient for  $\Delta E_{\Gamma L}$  needed to explain the temperature dependence of the Hall carrier

concentration. Aspnes reinterpreted the data of Blood<sup>21</sup> on the Hall coefficient measurement in *GaAs* using the  $\Gamma-L-X$  ordering of the conduction band minima and determined  $\Delta E_{\Gamma L}$  to be 0.28 eV at 650 K. The  $\Gamma-L$  energy separation of 0.28 eV in *GaAs* is in excellent agreement with the values of  $0.29 \pm 0.01$  eV (ref. 4) and 0.29 eV (ref. 19) for this separation at 300 K, determined respectively from the pressure dependence of the high field transport and capacitance measurements on Schottky diodes in *Ga<sub>1-x</sub>Al<sub>x</sub>As*. The  $\Gamma-L$  cross-over composition  $x = 0.47$  was found to be the same by Bhattacharya<sup>19</sup> and is in good agreement with the value  $x = 0.45 \pm 0.02$  (ref. 4). The sub-band-gap 0.205 eV for the  $L-X$  minima separation in *GaAs* is supported by the value 0.21 eV for this separation as obtained from the pseudopotential calculations<sup>22</sup>.

Onton *et al*<sup>23</sup> and Craford *et al*<sup>24</sup> measured the energy separation between the  $\Gamma-X$  minima in *GaAs* to be  $0.483 \pm 0.015$  eV at 2 K and 0.48 eV at 77 K, respectively, from the intraconduction band absorption in *GaAs* and measurement on the lowest absorption threshold in *GaAs<sub>1-x</sub>P<sub>x</sub>* alloys. The fact that although the  $L$  minima is lower than  $X$  in *GaAs*, the intraconduction band absorption measurements give the energy separation between the  $\Gamma-X$  minima, suggests that the  $\Gamma-L$  transitions are probably forbidden by the group theoretical selection rules. Aspnes obtained the best fit to the Hall coefficient data of Pitt and Less<sup>15</sup> for *GaAs* under pressure on the  $\Gamma-L-X$  ordering of the conduction band minima and using the same pressure coefficients for the  $\Gamma$ ,  $L$  and  $X$  minima as we have found for *Ga<sub>1-x</sub>Al<sub>x</sub>As*. This implies that the electrons in the  $\Gamma-L$  minima are principally involved in the current saturation effect<sup>4</sup> and that the direct-indirect cross-over of the lowest conduction band minima is  $\Gamma-X$  in *Ga<sub>1-x</sub>Al<sub>x</sub>As*. The Monte Carlo simulations<sup>13</sup> also show that the high field electron drift velocity in the  $L$  minima is much higher than in the  $X$  minima and that the electrons in the  $X$  minima contribute only about 10 per cent of the total conduction current. The  $\Gamma-L-X$  ordering of the conduction band minima established in the present work for alloy compositions  $0 < x < 0.37$ , resolves the apparent discrepancies in the sub-band-gaps as obtained from transport, photoemission and intraconduction band absorption measurements. Although the  $\Gamma-L-X$  ordering of the conduction band minima in *GaAs* was first proposed by Aspnes based on interpretation of the synchrotron-radiation Schottky barrier electroreflec-

tance spectra, application of the same interpretations does not yield the band structures of *GaP* and other semiconductors that are known from other well-established experiments<sup>25</sup>.

Littlejohn *et al*<sup>26</sup> showed that Monte Carlo calculations and experimental velocity field data<sup>27-29</sup> for *GaAs* are in agreement using the  $\Gamma-L-X$  conduction band ordering. The major parameter changes required from those used in previous  $\Gamma-X-L$  band ordering calculations to achieve this agreement are  $D_{\Gamma-L} = 1 \times 10^9$  eV/cm,  $D_{L-L} = 1 \times 10^9$  eV/cm and  $m_x^* = 0.58 m_0$  with a minimum  $\Gamma-L$  energy separation of 0.33 eV. The theoretically calculated luminescence efficiencies of *GaAs* and its alloys will be lowered by the  $L$  component of the wavefunctions of the electrons on the luminescent centres, which has been neglected in the past.

From the results shown in Fig. 5, it appears that the deep level follows the  $L$  minima at an energy of  $0.205 \pm 0.005$  eV for alloy composition in the range  $0.19 < x < 0.44$ . For  $x > 0.44$ , its activation energy below the  $X$  minima decreases with  $x$ , reaching a value of 0.106 eV at  $x = 0.78$ . The maximum activation energy of the deep level is 0.170 eV at  $x \approx 0.44$ . From the results shown in Fig. 3, it is also evident that the deep levels in *Ga<sub>1-x</sub>Al<sub>x</sub>As* are linked with the indirect minima. The binding energy of the deep level must, therefore, result from an interaction of the deep level potential with the conduction band minima at  $L$  and  $X$ . Since the electrons are very tightly bound in the deep states, an attempt has been made to calculate the deep level energy<sup>30</sup> in the 'tight binding approximation'. This is discussed elsewhere and the agreement between calculated and experimentally obtained activation energy of the deep level as a function of  $x$  is found to be satisfactory. Although shallow energy levels are present in the crystals, these are highly compensated by the acceptor impurities. The electrical properties of *Ga<sub>1-x</sub>Al<sub>x</sub>As* are, therefore, principally controlled by the deep levels. Since the electrons are very tightly bound in these deep states in *Ga<sub>1-x</sub>Al<sub>x</sub>As*, the carrier life times in the devices are expected to be adversely affected. The deep levels associated with subsidiary minima will also adversely affect the performance of LED's and lasers by providing nonradiative recombination process and transferring electrons to the deep levels. The deep levels have also been observed in intentionally doped *Ga<sub>1-x</sub>Al<sub>x</sub>As*<sup>9, 10, 30</sup> and in a number of other ternary alloys, such as *GaAs<sub>1-x</sub>*

$P_x^{31}$ ,  $Ga_x In_{1-x}P^{32}$ ,  $Ga_{1-x} In_x Sb^{33}$  and in  $Cd_{1-x} Zn_x Te^{34}$ . Louie *et al.*<sup>35</sup> have shown that the energy levels created by lattice vacancies are made up of valence band wavefunctions. The activation energy of the deep levels on such a model should, therefore, be independent of crystal composition. The results shown in Fig. 5 suggest that crystal defects in  $Ga_{1-x} Al_x As$  may be principally involved in creating deep levels, which may arise from a complex involving a native defect and an impurity.

An exact comparison between the deep level energy as a function of pressure and composition is not possible. This is due to the fact that the change in the band structure with alloy composition is not the same as with pressure. However, an approximate conversion from pressure to composition  $x$  is made by assuming linear variations of the  $\Gamma$  and  $X$  minima energies with  $x$  for  $0 < x < 0.43$ . The energy separation between the  $\Gamma$ - $X$  minima in  $GaAs$  is 0.485 eV at 300 K and the pressure coefficient for this separation is  $-14.1 \times 10^{-6}$  eV/bar. This gives a pressure of 39.4 k bar for the cross-over of the  $\Gamma$  -  $X$  minima, which is taken as equivalent to the composition  $x = 0.43$  when also the  $\Gamma$  -  $X$  minima are equal in energy. Thus, a conversion factor  $1.25 \times 10^{-2}$  per cent  $Al/k$  bar is obtained and is used to plot the deep level energy as a function of equivalent composition in Fig. 5.

The Hall to drift mobility ratio  $\mu_h/\mu_d$ , as shown in Fig. 6, attains a peak value of  $\sim 3.8$  for  $x \approx 0.42$  due to

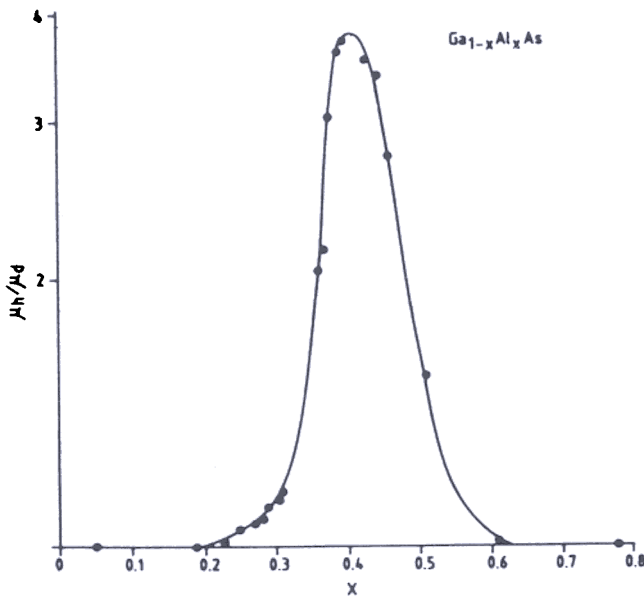


Figure 6. Hall to drift mobility ratio as a function of alloy composition at 300 K.

the multiconduction Hall effect. In  $GaAs$  and  $AlAs$ , a majority of the electrons occupy the lowest energy  $\Gamma$  and the  $X$  minima, respectively, and therefore,  $n_T \approx n_\Gamma \approx n_h$  ( $GaAs$ ) and  $n_T \approx n_X \approx n_h$  ( $AlAs$ ). Thus, the ratio  $\mu_h/\mu_d$  is close to unity for  $GaAs$  and  $AlAs$  from Eqn (7). As the alloy composition is increased, the energy separations between the  $\Gamma$  minimum and the subsidiary  $L$  and  $X$  minima decrease, thereby decreasing  $n_h$  because of electron transfer from the  $\Gamma$  minimum to the  $L$  and  $X$  minima. If there were no deep levels in the crystals,  $n_T$  will stay constant and, therefore,  $\mu_h/\mu_d$  will rise for increasing  $x$ . For alloy compositions  $x > 0.42$ , more electrons are transferred to the  $X$  minima, thereby increasing  $n_h$ , as result of which  $\mu_h/\mu_d$  decreases. The ratio  $\mu_h/\mu_d$ , therefore, attains a maximum around  $x \approx 0.42$ . Since there is a deep level in  $Ga_{1-x} Al_x As$  and its energy changes with  $x$ ,  $n_T$  does not stay constant as a function of  $x$ . The increased binding energy of the deep levels near the direct-indirect cross-over reduces the maximum value of the ratio  $\mu_h/\mu_d$  than what would have obtained without a deep level.

Majerfeld and Bhattacharya<sup>36</sup> have suggested and Saxena<sup>37</sup> has conclusively shown that electron capture and emission by the commonly observed 0.83 eV trap level in VPE and bulk  $GaAs$  occurs essentially via the  $L$  minima. It has also been shown<sup>38</sup> that electron capture and emission by the deep levels in  $Ga_{1-x} Al_x As$  occur via the  $L$  minima for  $0.25 < x < 0.32$  and via  $L$  and  $X$  for  $0.32 < x < 0.36$  (ref. 19). The persistent photoconductivity observed at low temperatures in  $Ga_{1-x} Al_x As$  crystals with direct band-gaps is, therefore, associated with the optically excited electrons from a level in the band-gap to the  $L$  minima, which rapidly thermalise in the  $\Gamma$  minimum and are prohibited from being recaptured by the deep level. The electron capture time by the deep level is  $\sim 1$  hour for  $T \leq 100$  K for  $x \approx 0.29$  (ref. 19), resulting in persistent photoconductivity. However, this model is inadequate to explain the persistent photoconductivity observed for crystals with as high a composition as  $x = 0.78$ , where the  $X$  minima is the lowest in energy and the deep level is principally associated with these minima. An increase in the photo-Hall mobility compared to the Hall mobility at low temperatures shows that an acceptor-like level is involved in photoexcitation. For crystals with indirect band-gaps, the small increase in  $n_h$  on photoexcitation at low temperatures shows that the electrons are excited from a level other than the deep level. The density of this level is found to increase with  $x$  for  $0.19 < x < 0.32$

and then decreases for  $x > 0.32$ . It may be that this level is created during the crystal growth and is associated with a crystal defect. A good agreement is found between  $\Delta N$  and  $\Delta N_1$  for  $x = 0.28$  and  $0.32$ , as found from the analysis of the temperature dependence of the Hall and photo-Hall carrier concentrations and mobilities respectively. The disagreement between  $\Delta N$  and  $\Delta N_1$  for  $x = 0.78$  may be due to the reason that the optically excited acceptor level has the properties of a double acceptor centre and the persistent photoconductivity is associated with the single charge state of this centre. A further increase in the photo-Hall mobility with white light at low temperature is found, showing that the deep level also has the properties of an acceptor-like centre. Nelson<sup>10</sup> showed that the deep levels in Te doped  $Ga_{1-x}Al_xAs$  have the properties of a donor level. The acceptor- or donor-like properties of the deep levels in  $Ga_{1-x}Al_xAs$  may, therefore, be related to the impurities incorporated in the layers during crystal growth. Nelson attributed the persistent photo-conductivity in  $Ga_{1-x}Al_xAs$  crystals to the large lattice relaxation of the donor levels. Since electron capture and emission by the deep levels in  $Ga_{1-x}Al_xAs$  occur via the indirect minima, there is no need to speculate the idea of a large lattice relaxation associated with the deep centres in  $Ga_{1-x}Al_xAs$ .

The low field properties reported here are very useful in knowing high field characteristics of devices. For example, the performance of Gunn diode made from  $GaAlAs$  will change with composition. One parameter of importance in many devices is the saturated high field velocity, which is normally derived from the measurement of current. The measured current cannot be converted into velocity until and unless the low field properties (particularly  $n_h$  and  $\mu_h/\mu_d$ ) are known in detail. This aspect of the present work will be reported elsewhere<sup>39</sup>.

## 6. CONCLUSIONS

It has been shown that the lowest indirect minima in  $Ga_{1-x}Al_xAs$  is  $L$  for alloy compositions in the range  $0 < x < 0.37$  and that the  $\Gamma-L$  cross-over composition is  $x = 0.47$ . It is concluded that principally the  $\Gamma$  and  $L$  minima are involved in any high field effect in  $GaAs$  and  $Ga_{1-x}Al_xAs$ . The  $\Gamma-L-X$  ordering of the conduction band minima in  $GaAs$  has resolved the discrepancies in apparent thresholds for the sub-band energy gaps as obtained from transport, photoemission and intraconduction band absorption measurements. The

energy separation between the  $\Gamma$  and  $L$  minima in  $GaAs$  is found to be  $0.280$  eV at  $300$  K. The electrical properties of  $Ga_{1-x}Al_xAs$  are controlled by the Saxena's deep levels associated with the indirect minima. The deep levels are found to have the properties of an acceptor-like centre. Another acceptor-like centre is also found in the alloy, which is probably associated with a crystal defect. The Hall to drift mobility ratio peaks near the direct-indirect cross-over composition and is found to be a factor of  $\sim 3.8$  for  $x \approx 0.42$ .

## ACKNOWLEDGEMENTS

The author wishes to thank Dr IGA Davies of STL for supplying  $Ga_{1-x}Al_xAs$  samples for this research. His thanks are also due to UK SRC for permitting the use of high pressure facilities at STL and University of Survey. He is thankful to the Government of India, the Universities of Sheffield and Roorkee and CSIR for support. I am indebted to Philips Research Lab, Netherlands for indentifying the deep level as Saxena's deep donor level<sup>40</sup>.

## REFERENCES

1. Neuberger, M. Handbook of electronic materials, Vol. 2, III-V Semi-conducting compounds. Plenum Press, New York, 1968. p.8.
2. Majerfeld, A. & Pearson, G.L. A high speed current limiting device from  $GaAs_{1-x}P_x$ . *IEEE Trans. Electron Devices*, 1967, **ED-14**(1), 632-37.
3. Immorlica, A.A. & Pearson, G.L. Velocity saturation in  $n$ -type  $Al_xGa_{1-x}As$  like single crystals. *Appl. Phys. Lett.*, 1974, **25**(10), 570-72.
4. Sugeta, T.; Majerfeld, A.; Saxena, A.K. & Robson, P.N. Velocity saturation and the conduction band structure of  $Ga_{1-x}Al_xAs$  under pressure. *Appl. Phys. Lett.*, 1977, **31**(12), 842-44.
5. Sitch, J.E.; Majerfeld, A.; Robson, P.N. & Hasegawa, F. Transit time induced microwave negative resistance in  $Ga_{1-x}Al_xAs - GaAs$  hetero-structure diodes. *Electron. Lett.*, 1975, **11**(19), 457-58.
6. Aspnes, D.E.  $GaAs$  lower conduction band minima: Ordering and properties. *Phys. Rev. B*, 1976, **14**(12), 5331-43.
7. Adams, A.R.; Vinson, P.J.; Pickering, C.; Pitt, G.D. & Fawcett, W. 3-level conduction band structure of  $GaAs$  from high stress and high field measurements. *Electron. Lett.*, 1977, **13**(2), 46-7.

8. Dingle, R.; Logan, R.A. & Arthur, J.R. The lower conduction band structure of  $Al_x Ga_{1-x} As$ . In Proceedings of 6th International Symposium on GaAs and related compounds, edited by C. Hilsum, Edinburgh, 20-22 Sept. 1976. Inst. of Phys. Conf. Ser. No. 33a, London, 1977. pp. 210-15.
9. Springthorpe, A.J.; King, F.D. & Becke, A. Te and Ge doping studies in  $Ga_{1-x} Al_x As$ . *J. Electron Matter*, 1975, **4**(1), 101-18.
10. Nelson, R.J. Long lifetime photoconductivity effect in *n*-type GaAlAs *Appl. Phys. Lett.*, 1977, **31**(5), 351-53.
11. Panish, M.B. Phase equilibria in the system Al-GaAs-Sn and electrical properties of Sn doped liquid phase epitaxial  $Al_x Ga_{1-x} As$ . *J. Appl. Phys.*, 1973, **44**(6), 2667-75.
12. Pitt, G.D. Hall effect measurements on single crystals at pressures extending upto 70 kb. *J. Phys. E*, 1977, **1**(2), 915-17.
13. Saxena, A.K. The conduction band structure and transport properties of  $Ga_{1-x} Al_x As$  alloys. University of Sheffield, Sheffield, 1978, PhD Thesis (unpublished).
14. Pitt, G.D. & Stewart, C.E.E. The electrical properties of  $GaAs_{1-x} P_x$  from a high pressure experiment. *J. Phys. C*, 1975, **8**(9), 1397-1411.
15. Pitt, G.D. & Lees, J. Electrical properties of the  $X_{1C}$  minima at low electric fields from a high pressure experiment. *Phys. Rev. B*, 1970, **2**(10), 4144-60.
16. Sze, S.M. Physics of semiconductor devices. Wiley Eastern Ltd., New Delhi, 1979. p. 743.
17. Aspnes, D.E. & Studna, A.A. Schottky barrier electroreflectance: Application to GaAs. *Phys. Rev. B*, 1973, **7**(10), 4605-25.
18. Epstein, A.S. Electron Scattering mechanisms in *n*-type epitaxial GaP. *J. Phys. Chem. Solids*, 1966, **27**(2), 1611-21.
19. Bhattacharya, P.K. Deep levels and the conduction band structure of GaAs and  $Ga_{1-x} Al_x As$ . University of Sheffield, Sheffield, 1978, PhD Thesis (unpublished).
20. James, L.W. & Moll, J.L. Transport properties of GaAs obtained from photoemission measurements. *Phys. Rev. B*, 1969, **183**(3), 740-53.
21. Blood, P. Electrical properties of *n*-type epitaxial GaAs at high temperature. *Phys. Rev. B*, 1972, **36**(6), 2257-61.
22. Chelikowsky, J.R. & Cohen, M.L. Nonlocal pseudopotential calculations for the electronic structure of eleven diamond and zinc-blende semiconductors. *Phys. Rev.*, 1976, **14**(2), 556-82.
23. Onton, A.; Chicotka, R.J. & Yacoby, Y. Subsidiary indirect conduction band minima and their donor levels in GaAs and InP. In Proceedings of the 11th International Conference on Physics of Semiconductors, Vol. 2 edited by M. Migsek. PWN Polish Scientific Publishers Warsaw, 1972. pp. 1023-29.
24. Craford, M.G.; Shaw, R.J.; Herzog, A.H. & Groves, W.O. Radiative recombination mechanisms in GaAs diodes with and without nitrogen doping. *J. Appl. Phys.*, 1972, **43**(10), 4075-83.
25. Cardona, M. Band structures of GaP and other semiconductors (unpublished).
26. Littlejohn, M.A.; Hauser, J.R. & Glisson, T.H. Velocity-field characteristics of GaAs with  $\Gamma_6^c L_6^c X_6^c$  conduction band ordering. *J. Appl. Phys.*, 1977, **48**(11), 4587-90.
27. Fawcett, W. & Herbert, D.C. High field transport in GaAs and InP. *J. Phys. C*, 1974, **7**(4), 1641-54.
28. Bosch, B.G. & Engelmann, R.W.H. Gunn effect electronics. Wiley, New York, 1975. p. 25 & 206.
29. Houston, P.A. & Evans, A.G.R. Electron drift velocity in *n*-GaAs at high electric fields. *Solid-State Electron.*, 1977, **20**(3), 197-204.
30. Kaneko, J.; Ayabe, M. & Watanabe, N. Electrical properties of *n*- $Al_x Ga_{1-x} As$ . In Proceedings of 6th International Symposium on GaAs and related compounds, edited by C. Hilsum. Institute of Physics, London, 1977. pp. 216-26.
31. Craford, M.G.; Stillman, G.E.; Rossi, J.A. & Holonyak Jr. N. Effect of Te and S donor levels on the properties of  $GaAs_{1-x} P_x$  near the direct-indirect transition, *Phys. Rev.*, 1968, **168**(3), 867-82.
32. Chevallier, J. Electrical properties of S doped  $Ga_x In_{1-x} P$  alloys. *Phys. Status Solidi b*, 1972, **14**(2), 531-39.

33. Campos D' Olne, M.; Gouskov A.; Gouskov, L. & Pons, J.C. Sulphur impurity state in  $Ga_{1-x}In_xSb$ . *Phys. Status Solidi b*, 1971, **47**(2), 137-41.
34. Lorenz, M.R.; Segall, B. & Woodbury, H.M. Some properties of a double acceptor centre in *CdTe*. *Phys. Rev.*, 1964, **134**(3A), A751-60.
35. Louie, S.G.; Schluter, M.; Chelikowsky, J.R. & Cohen, M.L. Self-consistent electronic states for reconstructed *Si* vacancy model. *Phys. Rev. B*, 1976, **13**(4), 1654-63.
36. Majerfeld, A. & Bhattacharya, P.K. New technique for identification of deep level trap emission to indirect conduction band minima in *GaAs*. *Appl. Phys. Lett.*, 1978, **33**(3), 259-61.
37. Saxena, A-K & Benyon, R.P. Characterization of bulk EL-2 trap in *GaAs* under hydrostatic pressure. *Proc. XIII AIRAPT Int. conf. on High Press. Science & Tech.* edited by A-K. Singh, Bangalore, 8-11 Oct. 1991. Oxford & IHB Publishing Co. Pvt. Ltd., New Delhi. 1992. pp 47-49.
38. Saxena, A-K. A search for resonant states from Saxena's deep levels in *GaAs* & *GaAlAs*: Evidence from Hall effect studies under hydrostatic pressure. *Semicond. Science & Tech.* (to be submitted).
39. Saxena, A.K. Calibration of  $I$ (vs  $E$ ) into  $v_d$  (vs  $E$ ) characteristics for  $Al_x Ga_{1-x} As$  alloys under hydrostatic pressure. *Electron. Lett.*, 1992 (submitted).
40. Henning, J.C.M.; Ansems, J.P.M. & Nijs, de A.G.M. Photoluminescence excitation of Saxena's deep donor in *AlGaAs*. *J. Phys. C. (Solid State Phys.)*, 1984, **17** (34), L915-21.